# CHARACTERISATION OF FRAGMENTATION CLOUDS AND FRAGMENTATION EVENT RECONSTRUCTION FOR SPACE BREAK-UP FORENSICS

**F. Ottoboni**(1), **C. Colombo**(1), **P. Grattagliano**(1), **A. Mignocchi**(1), **J.L. Gonzalo**(1), **A. Muciaccia**(1), **M.F. Montaruli**(1), **M. Maestrini**(1), **P. Di Lizia**(1), **L. Dimare**(2), **S. Cicalò**(2), **F. Guerra**(2), **F. Delfino**(2), **A. Rossi**(3), **X. Yan**(3), **M. Miklewski**(4), **F.J. Simarro Mecinas**(5), **L. Gisolfi**(6), **A. Horstmann**(7), **and T. Flohrer**(7)

(1) *Department of Aerospace Science and Technology, Politecnico di Milano, Via La Masa 34, 20156, Milan, Italy, Email: francesca.ottoboni@polimi.it, camilla.colombo@polimi.it, paola.grattagliano@polimi.it, alessandro.mignocchi@polimi.it, juanluis.gonzalo@polimi.it, andrea.muciaccia@polimi.it, marcofelice.montaruli@polimi.it, michele.maestrini@polimi.it, pierluigi.dilizia@polimi.it*

(2) *SpaceDyS S..r.l, Navacchio (PI), Italy, Email: dimare@spacedys.com, cicalo@spacedys.com, guerra@spacedys.com, delfino@spacedys.com*

(3) *IFAC-CNR, Via Madonna del Piano 10, 50019 Sesto Fiorentino (FI) Italy, Email: a.rossi@ifac.cnr.it, x.yan@ifac.cnr.it*

(4) *GMV Innovating Solutions Sp.z.o.o, Ul. Hrubieszowska 2, 01-209 Varsovia, Poland, Email: mmiklewski@gmv.com*

(5) *GMV, Isaac Newton, 11. P.T.M., 28760 Tres Cantos, Madrid, Spain, Email: fjsimarro@gmv.com*

(6) *Delft University of Technology, Faculty of Aerospace Engineering, Delft, The Netherlands, Email: L.Gisolfi@tudelft.nl*

(7) *European Space Agency, ESA-ESOC — Robert-Bosch-Strasse 5, DE-64293 Darmstadt, Germany, Email: Andre.Horstmann@ext.esa.int, Tim.Flohrer@esa.int*

## ABSTRACT

Space debris is a growing problem that threatens the safety and sustainability of space activities. Break-up events can occur due to collisions with other satellites or debris, as well as due to internal explosions within a satellite. In this context, the OFELIA tool is being devised to integrate in a unique tool the functionalities needed for on-orbit break-up reconstruction and characterisation. This work focuses on two main aspects of the tool: metrics for the cloud characterisation and observation capabilities and fragmentation reconstruction methods. Concerning the first aspect, several indicators related to the dynamics of the cloud of fragments are taken into account to characterise the short and medium terms evolution of cloud. The second aspect proposes to reconstruct in-orbit breakups in the short-term by considering two possible scenarios: the fragmentation is not known a priori, or there has been a fragmentation event alert and the involved objects are known.

Keywords: Fragmentation reconstruction, Breakup events, Debris cloud characterisation, Cloud observability metric.

## 1. INTRODUCTION

As the number of in-orbit space debris increases, the risk associated to possible breakup events is gaining relevance for the safety of space operations and active satellites. Fragmentations have been occurring in orbit since 1961 [1], due to catastrophic or non-catastrophic collisions between objects or to explosions of inactive satellites whose fuel reservoirs were not depleted [2], consequently further increasing the number of debris in orbit. Despite the adoption of collision avoidance manoeuvres, the data of the last 20 years showed that their number is growing. Indeed, the Cosmos 2251 and Iridium 33 collision of 2009 and the Fengyun 1C explosion of 2007 are among the most catastrophic events ever occurred, which lead to the generation of the highest number of catalogued fragments, making them the responsible for the biggest environmental impacts to date [3, 4].

For this reason, gaining insight into the dynamics of such events and their impact is essential, as their analysis for integration into space debris models and real-time operational assessments relies on several data sources. It is equally as important to be able to develop methods for the reconstruction of these events leveraging historical data to calibrate the models to be used for future analyses. This is the focus of the work in this paper, which describes the research performed within the European Space Agency (ESA)-funded project “T711-802SD – On-Orbit Breakup Forensics” by the consortium led by Politecnico di Milano, with the participation of GMV, Istituto di Fisica Applicata “Nello Carrara”, Consiglio Nazionale delle Ricerche and SpaceDyS. The activity is funded through ESA’s Technology Development Element and it is aligned with the objectives of ESA’s Space Safety Programme, focusing on the development of a unique tool - OFELIA (Orbital Fragmentation rEconstruction moduLe for forensIcs Analysis) - aimed at the detection, observation, characterisation and reconstruction of debris and the event which generated them. In particular, new methods were devised for the characterisation of debris

clouds, their observability and the reconstruction of occurred fragmentation events.
The paper is organised as follows. Section 2 introduces the OFELIA tool, with its general purpose. Section 3 describes the metrics developed for the characterisation of debris clouds and for their observability. Section 4 details the approach adopted for the reconstruction of fragmentation events, both when the event is known *a priori* and when it is not.

## 2. OFELIA TOOL

The OFELIA tool is a software prototype integrating all essential functionalities required for reconstructing and characterising on-orbit break-up events [5]. It is composed of a set of modules with different capabilities, which can work independently or in synergy to carry out several objectives, such as:

- contributing to bridging the gaps between the statistically modeled fragmentation cloud evolution and the measurements obtained by dedicated observation campaigns;
- providing improved modeling input from observational campaigns and deriving metrics to characterise the distribution of fragments and assess their observability by distributed sensors;
- developing a forensic assessment and observation planning prototype;
- improving the overall collision risk for short-term, but also medium- to long-term collision risk assessment;
- discriminating freshly generated debris clouds for enhancing sensor capabilities to detect individual fragments.

The tool will increase the confidence in the reconstruction of actual on-orbit breakup events from a limited and incomplete set of fragment data, it will characterise fragments by optimising the tasking of sensors and therefore will derive the detailed and revised risk assessments due to that fragmentation.
To ensure full functionality, OFELIA incorporates interfaces with existing ESA software. It is developed in Python and it is designed for use in a 64-bit Linux environment. The overall structure of the tool detailing the modules constituting the tool and their interactions and interfaces with respect to a full cycle of operations is described in [5].

The *fragmentation reconstruction and backward propagation module* identifies possible breakup events and estimates the epoch of the fragmentation. Moreover, it identifies the objects involved. The technical details of this module and the possible foreseen scenarios are detailed in Section 4.
The *break-up model module* aims at calibrating the POEM and COLBUSS [6] breakup models to improve the confidence of the simulation of fragmentation events.
The *cloud propagation model module* performs the propagation - both backward and forward - of the states of the objects in the analysis.
The *collision risk module* is necessary to produce the input for the ESA BUSTER tool, interfacing it with the cloud propagation module.
The *cloud expansion metric module* characterises the short and medium terms of the evolution of a debris cloud taking into account the statistical evaluation of the $\Delta V$s of the fragments and their orbital distribution with respect to the one of the parent, as well as the times for the formation of a torus and of a shell around the Earth. More details are given in section 3.1.
The *observability metric module* proposes to evaluate the observability of fragments by exploiting a Spatial Position Metric to assess the distribution of the observed fragments in space. To estimate the contribution that surveillance sensors can provide during the observation of the fragments cloud, a Resolution Capability Metric is also proposed. Further details are provided in section 3.2.
The *sensor tasking module* and *fragment characterisation module* provide fragments and sensor information observation request. These modules provide orbital information from observed data about the fragments to users and other subsystems.

## 3. METRICS FOR CLOUD CHARACTERISATION AND OBSERVATION CAPABILITIES

### 3.1. Fragmentation cloud characterisation

In order to properly reconstruct an in-orbit fragmentation it is important to fully characterise and understand the outcome of these type of events, studying both modelling and actual cases. Therefore, a number of fragmentations in different orbital regimes from Low Earth Orbit (LEO) to Geostationary Orbit (GEO) were simulated and some of the real events happened in the past decades were examined. Most of the simulations were performed using the NASA Breakup Model (BM) [7], with the aim to highlight some of its characteristics which could be of importance for the forensic analysis. A subset of cases were simulated using also the ESA COLBUSS fragmentation model [6]. At difference from the NASA BM the new model considers in detail the shape and composition of the target object. The analysis concentrated on the evaluation of the distribution of the changes in orbital elements (in particular, $\Delta a$, $\Delta e$ and $\Delta i$) among the fragments with the aim of assessing the region of the phase space where the search for fragments stemming from a given event should be conducted with the event reconstruction algorithms. Moreover, for the same purpose, methods to model and evaluate the spatial distribution and the timescales associated with the cloud evolution were devised. In the context of the present studies several simulations were performed using the NASA BM with the aim to highlight some of its characteristics which could be of importance for the forensic analysis.

Due to lack of space, it is not possible to report here all the results of the analysis. In an extreme synthesis, we can summarise the main findings as follows:

- the $\Delta V$ computed with the NASA BM (ranging from few m/s up to several tens of m/s for explosions....), especially in the collision cases, appear over estimated with respect to the ones observed in recent in-space fragmentations;
- the $\Delta V$ computed with the NASA BM is assumed to be isotropic, which is non optimal for energy reconstruction, especially in the case of collisions (see later in the text);
- despite the distinction present in the NASA BM between spacecraft (SC) and rocket bodies (RB), in absence of other data, from the distribution of the magnitude of the $\Delta V$s it would be very difficult to ascertain if a fragmentation was related to a SC or a RB;
- concerning the variation in orbital elements, in the NASA BM explosion cases in LEO, the $\Delta e$ values are generally limited below about 0.05 and most of the fragments are found within $\Delta i \sim \pm 1.6$ deg;
- the simulated explosions in Molnyia orbit show a significant dependence from the location of the event within the orbit (4 values of the mean anomalies were simulated). The distribution of the change in semimajor axis is significantly larger for the $M = 0$ case (explosion at perigee). This corresponds to the fact that an impulsive manoeuvre to increase the semimajor axis is more effective if performed at perigee. In the $M = 0$ case the $80^{th}$ percentile is found at $\Delta a = 907$ km, to be compared with, e.g., $\Delta a = 218$ km for the explosion happening at the apogee, $M = 180$ deg. The distributions of the $\Delta e$ are similar in the four cases. The two cases at 0 and 180 deg show a slightly larger spread (perigee or apogee manoeuvres are more suitable for a change in eccentricity). The i$\Delta e$ are confined within about $\pm 0.01$ for the $80^{th}$ percentile in all the 4 cases. As expected, the change in inclination is maximal, with a distribution much more spread, in the cases at 90 and 270 degrees, i.e., close to orbital nodes, reaching about $\pm 1$ degree for the $80^{th}$ percentile. In the other two cases the change in inclination is much lower and most of the orbits are found around $\pm 0.1$ deg. The case at $M = 0$, where the explosion happens at perigee, at a stronger gravity pull location, is the one with the smallest variations in inclinations;
- in the simulated collisions in LEO, with the NASA BM, the $\Delta a$ values for the RB case are much larger than those for the SC case. This might be an issue with the NASA BM model but, if physically sounding, could also be exploited in the forensic analysis. In any case the semimajor axis of the fragments span a significantly larger interval with respect to the target original value. Whereas negative values of $\Delta a$ are present, apparently the tendency is to have an increase in the semimajor axis. This characteristic shall be further investigated by comparing other fragmentation models and/or real data. The $\Delta e$ values are more homogeneous. The mean values are closer to the median and are generally limited below $0.1$. Once again, in the RB case the values are larger (about double) with respect to the SC case. The i$\Delta i$ values show a similar behaviour. Whereas in the SC case most of the fragments are found within about $\pm 2$ deg, in the RB case the interval spreads between about $\pm 4$ deg;
- for real events data, the TLE of the fragments from the Iridium-Cosmos collisions were analysed. It can be noticed how, despite the huge energy theoretically involved in the collision event, the change in inclinations is significantly lower than those predicted by the NASA BM. In particular, the $90^{th}$ percentile of the $\Delta i$ for the Iridium cloud is $0.133$ deg, while for the Cosmos cloud is $0.119$ deg. These values should be compared with those, about 10 times larger, for the simulated spacecraft case. Note also that this discrepancy might be related to a bias in the detection and cataloguing of the fragments. I.e., small fragments far from the target (in the orbital elements space) might not be catalogued and attributed properly to the Iridium-Cosmos event.

As mentioned above, once the orbital elements of some fragments are determined, the timescales of the cloud evolution processes can be estimated by considering the synodical period, $S$, of the fragments with respect to the one of the fragmented object:

$$\frac{1}{S} = \frac{1}{k}\left(\frac{1}{a_{\text{frag}}^{3/2}} - \frac{1}{a_{\text{parent}}^{3/2}}\right) \qquad (1)$$

where $k = \frac{2\pi}{\sqrt{GM}}$ and $a_{\text{frag}}$ and $a_{\text{parent}}$ are the semimajor axis of the fragment and of the parent object, respectively. Considering a cloud generated by typical spacecraft or rocket bodies fragmentations in highly inclined ($\sim 80°$) LEOs, at about 800 km of altitude, the $70^{th}$ percentile of the fragments' $S$, can be considered a reliable estimation of the formation time of the torus. This value ranges from $\sim$ 6 to $\sim$ 14 days (corresponding to $\sim$ 75 and $\sim$ 235 revolution of the parent object, respectively). Note that the typical $S$ periods for fragmentation in Highly Elliptical Orbits (HEOs), such as the Molniya ones, are $\sim$ 3 times longer in terms of days (while comparable if considered in units of the parent object orbital period).

Further on in the time evolution, the timescale for the formation of the shell around the altitude of the event, due to the spreading of the argument of the nodes caused by the perturbations related to the flattening of the Earth, can again be estimated simply by computing the synodical period of the nodal precession of the fragments with respect to the one of the fragmented object: $\frac{1}{S_\Omega} = \frac{1}{T_{\Omega_{\text{frag}}}} - \frac{1}{T_{\Omega_{\text{parent}}}}$, where $T_{\Omega_{\text{frag}}}$ and $T_{\Omega_{\text{parent}}}$ are the periods of the precessing node of the fragment and of the parent object's orbit, respectively. It can be assumed that the shell formation is reasonably completed once a given percentage (e.g., 70%) of the fragments have their node $180°$ apart from the precessing parent object, i.e., after half the full synodic period of the precession. The argument of perigee randomisation can be estimated with the same methodology. The timescale of the $\Omega$ randomisation, for a typical fragmentation in highly inclined ($\sim 80°$) LEOs, at about 800 km of altitude, is about $300 \div 350$ days (corresponding to $\sim 5000$ orbital periods of the parent object). The timescale for a similar event in HEOs (specifically Molniya orbits) is about 8 times longer due to the reduced $J_2$ effect, owing to the larger distance. The timescale for the $\omega$ randomisation in LEO is about half than the one for the argument of the node. Of course, being related to the $J_2$ effect, the timescale of the $\Omega$ and $\omega$ randomisation is strongly dependent on the orbital inclination of the parent object.

Finally, as it is well known, the NASA standard breakup model assumes an isotropic distribution of the $\Delta V$ imparted to the fragments. Whilst this is often a good approximation of a fragmentation, the analysis of the actual distribution of the $\Delta V$ vectors can give information on the real nature of the event. This can be performed by analyzing the eigenvalues and eigenvectors of the covariance matrix of the $\Delta V$ vectors. The direction of the eigenvector associated with the largest eigenvalue indicates the direction of maximum variance or spread. Hence, the ratio between the maximum and the minimum eigenvalues can be used as a metric to characterise the anisotropy of a given fragmentation. As expected, in the cases simulated with the NASA BM the ratio is always almost equal to 1, whereas the cases simulated with COLBUSS show interesting results according to the shapes of the simulated parent objects. The anisotropy algorithm shall be soon applied to data from real fragmentation events.

### 3.2. Observation capability metrics

In order to monitor and understand the dynamic evolution of fragment clouds resulting from fragmentation events, it is crucial to optimally task ground-based sensors. This requires establishing robust observation capability metrics that not only determine which sensors are best positioned to capture the highest number of fragments but also assess the unique contributions of each sensor in the monitoring network.
To this end, the proposed approach leverages two fundamental tools. First, the weighting factors of the Fragmentation Environmental Index (FEI) [8, 9, 10] are applied to derive a Spatial Position Metric (SPM). This metric provides a preliminary ranking by identifying,

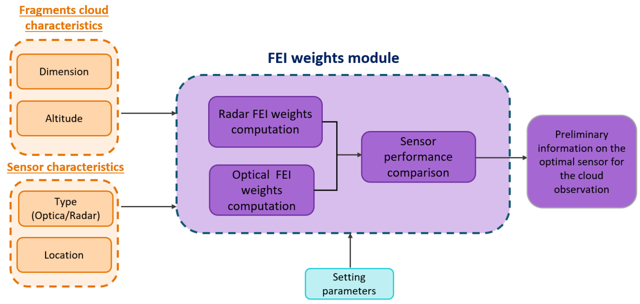


*Figure 1. Block diagram of the observability metric module.*

from a predefined set of sensors, those that are most likely to detect a maximum number of fragments based on their spatial positioning relative to the debris cloud.
Following this initial assessment, a detailed resolution analysis is conducted to compute the Resolution Capability Metric (RCM). The RCM quantitatively evaluates each sensor's ability to resolve individual fragments within its field of view (FoV) or within its field of regard (FoR), effectively classifying their observational performance. By statistically estimating the number of resolvable fragments, the RCM ensures that the sensor network can accurately track and distinguish closely spaced debris, thereby enhancing overall situational awareness.
This two-tiered methodology - employing the SPM for an efficient preliminary selection followed by the computationally intensive RCM for detailed performance evaluation - provides a comprehensive framework for sensor performance assessment during fragmentation events. Ultimately, it supports the strategic deployment of ground-based assets in space debris monitoring, ensuring both broad detection coverage and high-resolution fragment characterisation. The block diagram of the observability metric module is depicted in Figure 1.

#### Spatial Position Metric (SPM)

The first tool employed in the observation capability analysis is the Spatial Position Metric (SPM), which is derived from the novel FEI introduced by Gisolfi et al. [9, 8] to quantify and visualise the medium-term environmental effects of a fragmentation event in LEO. The FEI was originally developed to assess the impact of such an event on a space surveillance network, particularly considering that a significant number of fragments generated are too small to be detected by conventional Space Surveillance and Tracking (SST) sensors. This makes millimeter- and centimeter-sized debris particularly hazardous, as they cannot be tracked or avoided by active spacecraft.
To address this challenge, a multiplicative weight, denoted as $\omega_{\text{tr}}$, was introduced in a previous version of the metric [10] to enhance the significance of non-trackable objects. The updated formulation of the FEI is expressed

in Equation 2:

$$\Xi = \frac{M}{M_0}\frac{A}{A_0}\frac{D(h)}{D_0}\frac{L(h)}{L(h)0}f(i)\,\omega_{\rm tr}, \tag{2}$$

where $M$, $A$, and $L$ represent the mass, cross-sectional area, and lifetime of the object, respectively, and $D(h)$ denotes the spatial density. Among these components, the weight $\omega_{\rm tr}$ is particularly critical for debris cloud monitoring because it quantifies the increased risk associated with non-trackable fragments.

This weight is defined for both optical and radar sensors [11, 12], and serves as a preliminary indicator for evaluating whether an observing station is optimally configured to observe a specific fragment. Expanding this analysis to every visible fragment, the sensor's FoV or FoR allows to build a preliminary evaluation of the sensor coverage quality of the fragment cloud. In idealised scenarios, this index can be computed separately for purely optical or purely radar networks. However, in realistic operational environments — where both sensor types are available — the model computes $\omega_{\rm tr}$ for every fragment visible at the $k$-th epoch from the various sensors. These individual weights are then aggregated to form the final SPM, as expressed in Equation 3. This equation enables tracking of the time-varying performance of each sensor via the retrieval of $\mathrm{SPM}(t_k)$. When combined with a comprehensive visibility analysis, this approach implicitly ensures that the SST network consistently leverages the most suitable sensor for monitoring the fragment cloud at any given instant.

$$\mathrm{SPM}(t_k) = \sum_{i=1}^{N_{\text{frag}}} \omega_{{\rm tr},i}(t_k) \tag{3}$$

For optical sensors, the definition of $\omega_{\rm tr}$ is closely tied to the irradiance received from the object relative to the observing station, as well as to the object's angular velocity. In contrast, for radar sensors, $\omega_{\rm tr}$ is directly related to the fragment's Signal-to-Noise Ratio, which depends on parameters such as its altitude and physical size.

By analyzing the evolution of the SPM over time, it is possible to identify the operational windows during which a sensor exhibits optimal performance in tracking the debris cloud. This preliminary ranking not only facilitates the selection of a subset of sensors best suited for monitoring the fragmentation event but also paves the way for a more detailed, computationally intensive evaluation using the Resolution Capability Metric (RCM) on the selected subset.

**Resolution Capability Metric (RCM)**

After the preliminary sensor selection using the SPM, a more refined evaluation is conducted with the RCM to quantify the ability of the selected sensors to resolve individual fragments over time. In this analysis, a cloud of fragments whose evolution is modeled following the methodology described in [13] (or a similar source) is considered, and it is assumed that one of the sensors — either optical or radar — identified in the SPM analysis is available for tasking.

At a given $k$-th epoch, the sensor scans a total volume of the sky, denoted as $V_{\rm tot}$, proportional to its FoV or FoR. This volume gathers $N_s$ visible bins, each associated with a differential volume $\Delta V_{i,k}$, which represent discrete segments of the propagation model of the debris cloud.

For each bin, indexed by $i$, the fragment spatial density distribution, $\rho_{k,i}(A_{k,i})$, is computed as a function of the fragments size, $A_{k,i}$, by performing a linear regression on the discrete values of spatial density and area within that bin. In parallel, the minimum fragment size detectable by the sensor at the altitude corresponding to the $i$-th bin is determined according to the sensor's characteristics. Subsequently, the maximum fragment density in each bin is identified by examining the density corresponding to this minimum detectable size. The cumulative observable density in the bin $\rho_{k,i}^{cum}$ is then obtained by summing all the densities associated with fragments equal or larger than the minimum detectable size, and it is finally projected into the sensor's topocentric reference frame, effectively converting the three-dimensional (3D) spatial density into a two-dimensional (2D) density. In the next step, this 2D density is compared with the sensor's resolution limit. A resolution merit, $\xi_{k,i}$, is assigned — it is set to 1 if the density is within the sensor's resolution capability, and 0 otherwise. Next, for each visible bin, the cumulative detectable density is multiplied by the differential volume to determine the number of fragments detectable at the $k$-th observation epoch, $N^{\rm fg}(t_k)$, as in Equation 4. This quantity serves as the key figure of merit for the RCM, as it encapsulates the sensor's fragment detection potential over time.

$$\begin{aligned}\mathrm{RCM}(t_k) = N^{\rm fg}(t_k) &= \sum_{i=1}^{N_s} N^{{\rm fg},i}(t_k) \\ &= \sum_{i=1}^{N_s} \rho_{k,i}^{cum}\,\Delta V_{i,k}\end{aligned} \tag{4}$$

Together, the resolution merit $\xi_{k,i}$ and the number of detectable fragments $N^{\rm fg}(t_k)$ serve as key performance metrics for the sensor at the $k$-th epoch. By evaluating these metrics over successive epochs, a time-varying performance profile of the sensor is constructed, as depicted in Figure 2. This profile facilitates the assessment of which sensors, from the subset pre-selected via the SPM analysis, are most likely to detect the maximum number of objects, ensuring that the most suitable sensor is leveraged for monitoring the evolving debris cloud.

## 4. FRAGMENTATION RECONSTRUCTION METHODS

The aim of the backward propagation and fragmentation reconstruction module is the detection and characterisation of a fragmentation event *a posteriori*, starting from available Two-Line-Element (TLE) data. This allows for a fast evaluation of the potential consequences of

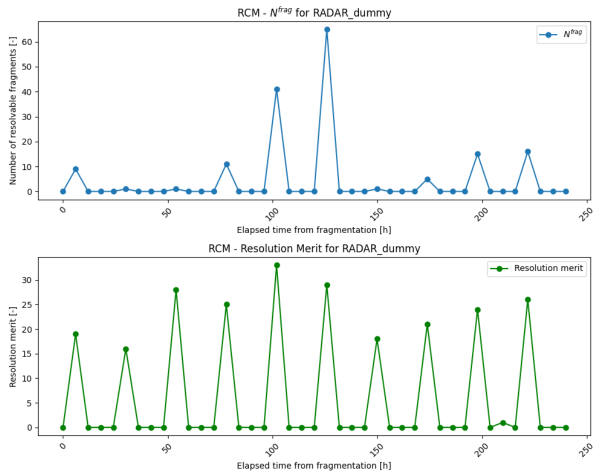


*Figure 2. Example of evolution in time of the RCM resolvable number of fragments ($N^{\mathrm{fg}}$) and resolution merit ($\xi$) for a radar sensor observing a fragment cloud.*

a breakup in terms of collision risk posed to other active satellites and for swift operations for tasks such as collision avoidance manoeuvres and observation planning. The crucial information retrieved from the reconstruction includes the objects involved in the event, i.e. the cataloged fragments and the parent(s) which generated them, as well as the epoch of the event.
Several techniques were devised in the past with this objective, such as the method based on similarity distance functions between the orbital elements of the objects under analysis by Dimare et al. [14] or the Simulation of On-Orbit Fragmentation Tool (SOFT) by Andrisan et al. [15], which exploits the average distance between objects in a debris cloud, identifying the time of the minimum average distance and the position of the center of mass of the cloud as the time and position of the breakup. Celletti et al. [16] instead developed a technique to match debris objects to their parents by exploiting the proper elements of the objects and propagating backward. At Politecnico di Milano, two main approaches were developed. The PUZZLE approach [17, 18] is based on the backward propagation of the orbital elements of the objects coupled with pruning and clustering techniques to identify families of objects and match them to their parent, while the Fragmentation Epoch Detector (FRED) method [19] relies on a stochastic approach to select the fragmentation epoch candidates by exploiting the Minimum Orbital Intersection Distance (MOID) computation.
The method proposed in the OFELIA module for fragmentation reconstruction is based on the works in [17, 19], unifying them into a single modified approach to increase the robustness of the reconstruction. The method is able to reconstruct the event in two scenarios: when the event is known, i.e. the generated fragments are known and so is the parent, and when the event is not known, i.e. the parent is unknown and it is uncertain which objects were generated. The user inputs which scenario is analysed, and the algorithm then branches accordingly, following different procedures. This approach exploits

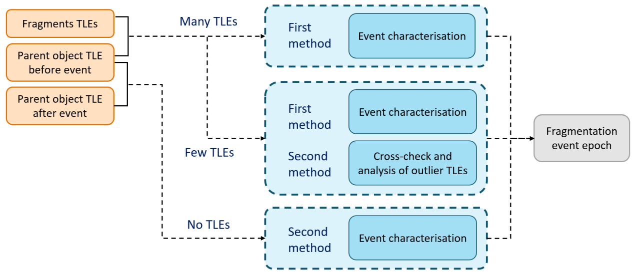


*Figure 3. Block diagram of the fragmentation reconstruction approach when the fragmentation is known.*

the backward propagation carried out with SGP4 propagator [20], whose accuracy limits the analyses to about two weeks after the event, therefore the whole method is employed for the short-term reconstruction of a breakup.

### 4.1. Fragmentation is known

When the fragmentation is known, the parent object and the generated fragments are established *a priori*, hence the method receives as input the TLEs of these objects. For this reason, the fragmentation reconstruction focuses on the estimation of the epoch of the breakup event, and does not perform the steps required for the pruning of the initial data, which are considered certain. The clustering of objects into fragments families is also skipped, as the fragments given as inputs are assumed to be a single family generated in the event.
The approach reads the input TLEs, and depending on their number it applies one of two methods. The block diagram of the approach is shown in Figure 3.

The first method, which is used a stand-alone when a sufficiently high number of TLEs are available, is based on the work in [17]. The first step consists in processing the TLEs according to the SGP4 framework and selecting a single TLE for each object. Then, a triple-loop filter based on the one of Hoots et al. [21] is applied to the objects taken in pairs. The triple-loop filter relies on the sequential application of two geometrical filters and a temporal one. The first filter is an apogee-perigee pruning step, whose objective is to assess the geometrical compatibility of the orbits of the objects. Indeed, it compares the maximum of the two perigees and the minimum of the two apogees of the couple of objects under analysis to verify that their difference is below a given threshold, which is an input to the method. In the positive instance, the two objects pass the filter. The second pruning step is a MOID filter, which computes the MOID between the two objects according to the analytical formulation by Gronchi [22] and verifies that it is below the given threshold, which implies that the close approach between the objects is deemed possible. If the objects do not pass the filter, they are discarded from the analysis. The last step is a temporal filter, which first selects angular windows around the MOID and then converts them into temporal windows, to check whether two objects were in the same angular window at the same time, which is the necessary condition for a close approach. Since the input objects are known to be generated in the event, it is expected that in this scenario all input objects pass the triple-loop filter. The triple-loop filter is coupled with a backward propagation in a given time window which is an input to the approach, and an iterative computation of the time and distance of close approach for each pair of objects is performed. The propagation exploits the SGP4 propagator, hence osculating orbital elements are considered. The epoch of the event is identified by this method as the temporal bin with the highest density of close encounters between the objects.

When only a limited number of TLEs are available, the reliability of the first method decreases, as the identified close encounters are insufficient to accurately determine the fragmentation epoch. For this reason, in this instance the first method is coupled with a second method to increase the robustness of the estimation of the fragmentation epoch. The second method is based on the tool presented in [19], with a modification in the algorithm introduced to add reliability in the computation of the candidate fragmentation epochs. As in [19], the second method starts from the fragment(s) orbital state derived from the TLE (the mean state) to which a synthetic covariance is associated, and from the last available TLE of the parent object (assumed as deterministic). The fragment orbital state is populated with a multivariate normal distribution to generate Monte Carlo samples. For each couple sample-parent, the epochs of parent transit through the MOID [22] are computed on a time window. This window is defined as the interval of time going from the epoch of the last available parent TLE up to 10 days, with a step equal to the parent orbital period. The MOID computed according to [22] is iteratively refined to account for perturbations considered in the SGP4 model, used to propagate the objects dynamics. Subsequently, differently from the original version of FRED in [19], the epochs of passage through the MOID are not yet considered as the fragmentation epoch candidates. Indeed, instead, the transit epochs through the inertial MOID points are refined through an optimisation algorithm which computes the Times of Closest Approach (TCAs). This computation is carried out by considering the epoch of parent transit through the MOID as TCA first guess, for each time interval in the window, between the parent and sample fragment. This guess of TCA is refined by searching for the epoch of the minimum relative distance $\boldsymbol{r}_{rel}$ between the parent and sample fragment orbital states along the time window, by applying Equation 5.

$$\frac{d}{dt}(\boldsymbol{r}_{rel} \cdot \boldsymbol{r}_{rel}) = 0 \tag{5}$$

Equation 5 is verified when the relative distance is orthogonal to the relative velocity between the two objects, hence providing with Equation 6, solved iteratively.

$$\boldsymbol{r}_{rel} \cdot \boldsymbol{v}_{rel} = 0 \tag{6}$$

In this way, a set of TCA epochs for each couple parent-sample is retrieved along the time intervals inside the time window of analysis. The set of TCA epochs undergoes a filtering process in order to eliminate outliers, and is then clustered in time, returning fragmentation epoch candidates. For each cluster, both the three-dimensional MOID and the three-dimensional relative distance distributions are derived. Given that, at the actual fragmentation epoch, the MOID and relative distance were equal, the fragmentation epoch candidates are ranked according to the stochastic matching between the two distributions. To assess such a compliance, the two distributions are first rotated in curvilinear coordinates [23]. The Earth Moving Distance (EMD) metric [24], which applies also for any kind of distribution (including non-Gaussian), can then be used to compute the statistical distance between the distributions. Therefore, the fragmentation epoch candidates are ranked based on this statistical distance, and the candidate featuring the smallest EMD is finally selected. Thus, an estimated epoch of the break-up event is returned by the second method, together with its mean and standard deviation. The last foreseen scenario when the fragmentation is known is the case where no fragment TLE is available, yet the parent object which fragmented is known and two of its TLEs are available. In particular, these TLEs are assumed to be related to the parent object, one at an epoch slightly before the event and one at an epoch that is subsequent to the event. Here, the second method is applied exactly as described above, but the fragment orbital state is replaced with the orbital state of the parent object extracted from the TLE temporally located after the event (the second TLE mentioned above). The estimated fragmentation epoch and the associated uncertainty are thus available even if only the orbital data of the parent object are available.

### 4.2. Fragmentation is unknown

When the fragmentation event is unknown, it is assumed that the input data set includes both the fragments resulting from the event and unrelated external objects. The specific fragments produced by the fragmentation, as well as their parent object, are not identified *a priori*. Therefore, the focus of the fragmentation reconstruction method in this case is the identification of the objects involved in the fragmentation event, i.e. the families of fragments and the related parent(s), as well as the estimation of the fragmentation epoch.

The block diagram for the approach adopted in this scenario is in Figure 4. In this scenario, the input TLEs are read and processed according to the SGP4 framework, then they are pre-filtered to look for possible statistical outliers exploiting the filters developed by Lidtke et al. [25]. As in the previous scenario, a single TLE per object is selected and the triple-loop filter is applied to each pair of objects. As opposed to the first scenario, this procedure is necessary before the branching of the algorithm depending on the number of TLEs because not all input objects were part of the fragmentation event, and the triple-loop filter selects only those for which a close approach was possible. This filtering process ensures that the objects retained for further analysis are those most likely originating from the fragmentation event. In this way, the algorithm adapts its approach according to the

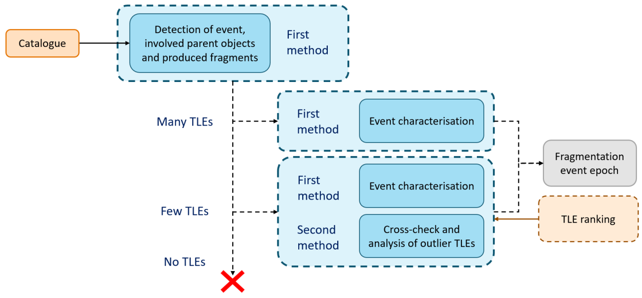


*Figure 4. Block diagram of the fragmentation reconstruction approach when the fragmentation is not known.*

number of available TLEs of these objects. As in the known fragmentation case, if a sufficiently high number of TLEs is available the first method, based on the work in [17], is applied.
In this scenario, the fragmentation epoch is estimated with the same binning approach as in the previous case. However, instead of halting the analysis when the epoch is found, the process continues and looks for clusters of objects. A cluster is identified as a family of objects (fragments) which likely share a common origin by using the Hierarchical Clustering Method (HCM) proposed by Zappalà et al. [26], which was already employed to find families of asteroids. As in [17], the method was modified so that it assigns a distance function $\delta v$ to pairs of objects to measure their separation, taking into account osculating orbital elements and considering also the right ascension of the ascending node ($\Omega$) and the argument of pericenter ($\omega$) on top of the semi-major axis ($a$), inclination ($i$) and eccentricity ($e$). The final expression for the distance function is given by:

$$\delta v = na\left[k_1\left(\frac{\delta a}{a}\right) + k_2(\delta e)^2 + k_3(\delta i)^2 + k_4(\delta\Omega)^2 + k_5(\delta\omega)^2\right]^{1/2} \tag{7}$$

where $n$ is the mean motion and the $k_j$ coefficients are of the order of unity, depending on each parameter to which they are associated.

Once the families of objects are identified, the average distance among the objects of each family is computed, to verify that it is below a given threshold, hence that it is compatible with a fragmentation event. The last step of the method compares the position of the fragments with the position of known cataloged objects, identifying the parent as the closest object to the cluster.
If after the triple-loop step the approach identified a number of TLEs belonging to the event which is not sufficient to apply the first method alone with high reliability, both the first and second methods are adopted sequentially. However, to increase the accuracy of the final result of the analysis, after the application of the first method a ranking of the TLEs of the objects that were identified as part of the event is carried out. The ranking is based on the computed miss distance at the time of the fragmentation, i.e. it is assumed that the smaller the miss distance the higher the probability that the object was generated in the fragmentation event. Thus, the five objects with the smallest miss distance are selected and given as input to the second method, together with the TLE of the parent that was identified. The second method is applied exactly as described in Section 4.1, with the difference that the inputs on the parent and fragment orbital states are provided by the first method, as mentioned above.

### 4.3. Application to a real fragmentation event

The fragmentation reconstruction module of OFELIA is applied to the breakup event of the Chinese Long March 6A rocket's upper stage, whose explosion occurred on 12/11/2022. The objective of this section is to evaluate the accuracy of the approach in reconstructing both the epoch of the event and the objects involved. To this aim, the foreseen scenario is the one in which the fragmentation is not known, i.e. the input TLE file is composed of TLEs of the fragments (and the parent) as well as of other unrelated objects. This allows to assess whether the pruning process works properly as the objects involved in the event are not assumed *a priori*.
The input file is composed of 61 TLEs belonging to 43 objects, of which 31 are CZ6A fragments, downloaded from SpaceTrack [27] and dated ten days after the event. After the application of the pre-filtering process, 7 outliers are discarded. The set of objects with potential close encounters is determined after applying the triple-loop filter, which retains 34 objects for analysis. Among them, 31 are CZ6A fragments, indicating that the triple-loop filter successfully preserved all of the relevant objects. With the amount of objects in the analysis, both the first and the second methods are applied to increase the reliability of the reconstruction. The main results of the first method are reported in Table 1, while the results of the second method are in Table 2.

*Table 1. CZ-6A fragmentation reconstruction results with first method.*

| | |
|---|---|
| Initial size of TLE set | 61 |
| Search window | 14 days |
| Estimated fragmentation epoch | 12/11/2022 05:26:39 UTC |
| Number of involved objects | 25 |
| Identified parent | CZ6A NORAD: 54236 |

Both methods identify the correct fragmentation epoch, placing it on 12/11/2022. The first method assesses the time of the event as 05:26:39, while the second places it between around 03:45 and 7:10, with the second ranked result being about 5:30 hence confirming the estimate of

Table 2. *CZ-6A fragmentation reconstruction results with second method (1000 samples).*

| Fragment | Score | Epoch | Std deviation [s] |
|---|---|---|---|
| 1 | 1.0 | 2022-11-12 03:46:17.2319 | 1.7881e-07 |
| | 0.988392 | 2022-11-12 05:28:13.7216 | 0.0 |
| | 0.977643 | 2022-11-12 07:10:13.4519 | 1.7881e-07 |
| 2 | 1.0 | 2022-11-12 03:49:32.7003 | 1.7881e-07 |
| | 0.927923 | 2022-11-12 05:29:22.9968 | 1.1921e-07 |
| | 0.853037 | 2022-11-12 07:09:32.9434 | 1.7881e-07 |
| 3 | 1.0 | 2022-11-12 03:49:08.1634 | 5.9605e-08 |
| | 0.891975 | 2022-11-12 05:30:41.8258 | 1.7881e-07 |
| | 0.816621 | 2022-11-12 07:12:19.4940 | 5.9605e-08 |
| 4 | 1.0 | 2022-11-12 03:48:00.2201 | 5.9605e-08 |
| | 0.991297 | 2022-11-12 05:29:40.3245 | 0.0 |
| | 0.982887 | 2022-11-12 07:11:21.4967 | 2.3942e-07 |
| 5 | 1.0 | 2022-11-12 03:44:52.2373 | 1.1921e-07 |
| | 0.983155 | 2022-11-12 05:26:42.8382 | 1.7881e-07 |
| | 0.965586 | 2022-11-12 07:08:30.7497 | 2.3842e-07 |

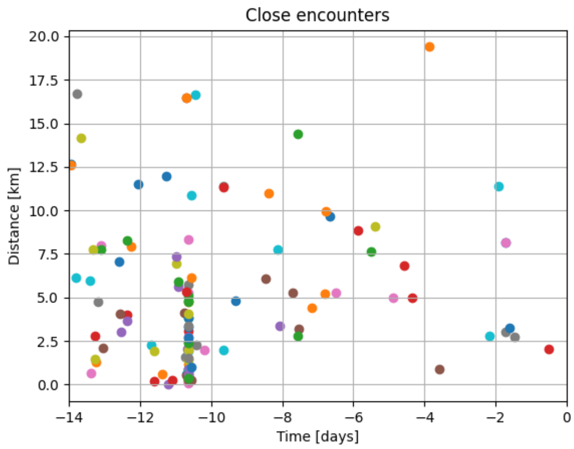


*Figure 5. Close approach distance with respect to time of the fragmentation search computed by the first method.*

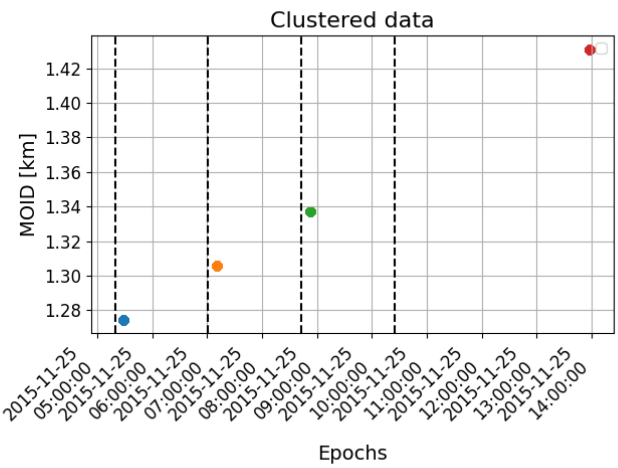


*Figure 6. Clustered fragmentation epoch candidates with the corresponding MOID distances computed by the second method.*

the first method. Figure 5 shows the close encounter distance with respect to the temporal window in which the fragmentation is searched for each pair of objects under analysis as computed by the first method. The clear concentration of close encounters at about eleven days before the epoch of the TLEs indicates the presence of a breakup event. Figure 6 shows the MOID distances with respect to the clusters of fragmentation event candidate epochs for each time interval of the analysis window, as computed by the second method, for one of the fragments TLEs analysed. It is evident that the first cluster (the blue samples) is related to candidate epochs which are in the surroundings of the epoch estimated by the first method (Table 1), hence confirming the results of this fragmentation reconstruction.

The first method is capable of identifying the correct parent object, as visible in Table 1, which is then fed into the second method. Moreover, 25 objects are recognised as fragments due to the fragmentation event out of 31 - although one is actually detected as the parent object, therefore the actual fragments are 30 - leading to the correct classification of 81% of the input fragments.

## 5. CONCLUSIONS

The increase in the number of space debris, and consequently of fragmentation events is occurring at an alarming rate for the sustainability of space operations. In this context, the OFELIA tool is designed to perform a full cycle of operations from the characterisation of the fragments from the processing of observations, going on with the break-up reconstruction, the simulation of the full cloud of fragments, the forward propagation of it, the characterisation of the cloud expansion, and the optimisation of tasking observations for subsequent observations. Three sub-modules of OFELIA were described in detail. For the characterisation of fragmentation clouds, several fragmentation events in different orbital regimes were analysed, both with real and simulated data with the NASA Breakup model and the ESA COLBUSS model. Interesting insights were drawn on the reliability of these models with the aim of a forensic analysis on the occurred breakups, highlighting both useful features of the models and possibly problematic ones. The complete characterisation of breakup events exploits not only the cloud evolution process, but also two different metrics concerning the observation capability of fragments, which is the focus of the observability metric module. To assess the best sensors for a given fragmentation event, a Spatial Position Metric is devised, which is coupled with a Resolution Capability Metric to quantify the ability of such sensors to resolve individual fragments over time. Lastly, the investigation of a breakup event encompasses also its reconstruction in terms of epoch and objects involved. The fragmentation reconstruction module uses a backward propagation of the fragments coupled with pruning and clustering techniques as well as a stochastic approach based on the computation of the MOID to increase the reliability of the reconstruction. The module is able to investigate both known breakup events, for which information is available regarding the parent object(s), and unknown events. Moreover, its application to well known fragmentation events gave satisfactory results.

## ACKNOWLEDGMENTS

This project has received funding from the European Space Agency contract 4000143257/23/D/SR for the project "T711-802SD – On-Orbit Breakup Forensics". X.Y. acknowledges funding from the Italian Space Agency (ASI Contract "Detriti Spaziali - Supporto alle attività IADC e SST 2023-2025").

## REFERENCES

1. Anz-Meador, P. D., Opiela, J. N., Shoots, D., and Liou, J.-C., "History of On-orbit satellite fragmentations $15^{th}$ Edition," *National Aeronautics and Space Administratio, Lyndon B. Johnson Space Center,Houston, Texas 77058*, 2018.
2. "ESA'S annual Space Environment Report," Tech. rep., ESA, ESOC, 2024, No. GEN-DB-LOG-00288-OPS-SD.
3. Anselmo, L. and Pardini, C., "Analysis of the consequences in low Earth orbit of the collision between Cosmos 2251 and Iridium 33," *Proceedings of the 21st international symposium on space flight dynamics*, Vol. 294, Centre nationale d'etudes spatiales Paris France, 2009.
4. Pardini, C. and Anselmo, L., "Assessment of the consequences of the Fengyun-1C breakup in low Earth orbit," *Advances in Space Research*, Vol. 44, 9 2009, pp. 545–557.
5. Colombo, C., Gonzalo Gomez, J., Ottoboni, F., Giudici, L., Muciaccia, A., Grattagliano, P., Mignocchi, A., Montaruli, M., Di Lizia, P., Maestrini, M., et al., "On-Orbit Breakup Forensics: Analysis of Measurement Data to Reconstruct Fragmentation Events in Space," *75th International Astronautical Congress (IAC 2024)*, Milan, Italy, 2024, pp. 1–14.
6. Dimare, L., Francesconi, A., Giacomuzzo, C., Cicalò, S., Rossi, A., Olivieri, L., Sarego, G., Guerra, F., Lemmens, S., and Braun, V., "Advances in the characterisation of collision break-ups by means of numerical modelling," *Proceedings of the* $72^{nd}$ *International Astronautical Congress*, Vol. Paper IAC-21,A6,3,6,x65067,, Dubai, United Arab Emirates, 2021.
7. Johnson, N. L., Krisko, P. H., Liou, J. C., and Anz-Meador, P. D., "NASA's new breakup model of EVOLVE 4.0," *Advances in Space Research*, Vol. 28.9, 2001, pp. 1377–1384, doi:10.1016/S0273-1177(01)00423-9.
8. Gisolfi, L., Rossi, A., and Marzari, F., "Fast characterization of in-orbit fragmentations," *Proceedings of the International Astronautical Congress, IAC*, Vol. IAC-24,A6,7,x85251, Milan, Italy, 2024.
9. Gisolfi, L., Marzari, F., and Rossi, A., "An Upgraded Environmental Index for the SST Fragmentation Service," *Proceedings of the 2nd Orbital Debris Conference*, Vol. 2852 of *LPI Contributions*, Texas, USA, 2023, p. 6038, Paper 6038.
10. Rossi, A., Vellutini, E., Alessi, E., Schettino, G., Ruch, V., and Dolado Perez, J., "Environmental index for fragmentation impact and environment evolution analysis," *Journal of Space Safety Engineering*, Vol. 9, 2022, pp. 269–273.
11. Bonaccorsi, S., Montaruli, M. F., Di Lizia, P., Peroni, M., Panico, A., Rigamonti, M., and Del Prete, F., "Conjunction Analysis Software Suite for Space Surveillance and Tracking," *Aerospace*, Vol. 11, No. 2, 2024, pp. 122.

12. Bianchi, G., Mariotti, S., Montaruli, M. F., Di Lizia, P., Massari, M., De Luca, M. A., Demuru, R., Sangaletti, G., Mesiano, L., and Boreanaz, I., "The New Transmitting Antenna for BIRALES," *Aeronautics and Astronautics: AIDAA XXVII International Congress*, 4-7th September 2023, Padova, Italy, 2023.

13. Giudici, L., Trisolini, M., and Colombo, C., "Probabilistic Multi-Dimensional Debris Cloud Propagation Subject to Non-Linear Dynamics," *Advances in Space Research*, Vol. 72, No. 2, 2023, pp. 129–151.

14. Dimare, L., Cicalò, S., Rossi, A., Alessi, E. M., and Valsecchi, G. B., "In-orbit fragmentation characterization and parent bodies identification by means of orbital distances," *First International Orbital Debris Conference*, Dec. 9-12 2019, Sugarland, Houston, TX, USA.

15. Andrisan, R. L., Ionită, A. G., González, R. D., Ortiz, N. S., Caballero, F. P., and Krag, H., "Fragmentation Event Model and Assessment Tool (Fremat) Supporting on-Orbit Fragmentation Analysis," *7th European Conference on Space Debris*, Apr. 17-21 2017, Darmstadt, Germany.

16. Celletti, A., Pucacco, G., and Vartolomei, T., "Reconnecting groups of space debris to their parent body through proper elements," *Scientific Reports*, Vol. 11, No. 1, 2021, pp. 22676.

17. Romano, M., Muciaccia, A., Trisolini, M., Lizia, P. D., Colombo, C., Alessandra, D. C., and Salotti, L., "Characterising in-orbit fragmentations with the PUZZLE software," *8th European Conference on Space Debris*, Apr. 20-23 2021, Darmstadt, Germany.

18. Muciaccia, A., Romano, M., Trisolini, M., and Colombo, C., "Reconstruction of in-orbit breakup events over the long term," *Acta Astronautica*, Vol. 228, 3 2025, pp. 875–885.

19. Montaruli, M. F., Lizia, P. D., Cordelli, E., Ma, H., and Siminski, J., "A stochastic approach to detect fragmentation epoch from a single fragment orbit determination," *Advances in Space Research*, Vol. 72.9, 2023, pp. 3713–3733, doi:10.1016/J.ASR.2023.08.031.

20. Vallado, D. A., Crawford, P., Hujsak, R., and Kelso, T. S., "Revisiting Spacetrack Report #3," *AIAA/AAS Astrodynamics Specialist Conference and Exhibit*, 21-24 Aug. 2006, Keystone, Colorado. doi:10.2514/6.2006-6753.

21. Hoots, F. R., Crawford, L. L., and Roehrich, R. L., "An analytic method to determine future close approaches between satellites," *Celestial Mechanics*, Vol. 33, 1984, pp. 143–158, doi:10.1007/BF01234152.

22. Gronchi, G. F., "An algebraic method to compute the critical points of the distance function between two Keplerian orbits," *Celestial Mechanics and Dynamical Astronomy*, Vol. 93, 2005, pp. 295–329, doi:10.1007/s10569-005-1623-5.

23. Vallado, D. A. and Alfano, S., "Curvilinear coordinate transformations for relative motion," *Celestial Mechanics and Dynamical Astronomy*, Vol. 118, No. 3, 2014, pp. 253–271.

24. Levina, E. and Bickel, P., "The earth mover's distance is the mallows distance: Some insights from statistics," *Proceedings Eighth IEEE International Conference on Computer Vision. ICCV 2001*, Vol. 2, IEEE, 2001, pp. 251–256.

25. Lidtke, A. A., Gondelach, D. J., and Armellin, R., "Optimising filtering of two-line element sets to increase re-entry prediction accuracy for GTO objects," *Advances in Space Research*, Vol. 63, 2019, pp. 1289–1317, doi:10.1016/j.asr.2018.10.018.

26. Zappala, V., Cellino, A., Farinella, P., and Knezevic, Z., "Asteroid families. I - Identification by hierarchical clustering and reliability assessment," *The Astronomical Journal*, Vol. 100, 1990, pp. 2030–2046, doi:10.1086/115658.

27. SpaceTrack. Consulted on 18 February 2025. https://www.space-track.org/.